Available online at www.sciencedirect.com
SCIENCE DIRECT®
Nuclear Instruments and Methods in Physics Research B 247 (2006) 31–37
NIM B
Beam Interactions with Materials & Atoms
www.elsevier.com/locate/nimb

Application of the zero-range potential model to positron annihilation on molecules

G.F. Gribakin *, C.M.R. Lee

Department of Applied Mathematics and Theoretical Physics, Queen's University Belfast, Belfast BT7 1NN, Northern Ireland, UK

Available online 9 March 2006

Abstract

In this paper we use a zero-range potential (ZRP) method to model positron interaction with molecules. This allows us to investigate the effect of molecular vibrations on positron–molecule annihilation using the van der Waals dimer Kr_2 as an example. We also use the ZRP to explore positron binding to polyatomics and examine the dependence of the binding energy on the size of the molecule for alkanes. We find that a second bound state appears for a molecule with ten carbons, similar to recent experimental evidence for such a state emerging in alkanes with twelve carbons.

PACS: 34.85.+x; 78.70.Bj; 34.10.+x; 34.80.Gs

Keywords: Positron–molecule collisions; Annihilation; Vibrational Feshbach resonances; Bound states

1. Introduction

The main aim of this work is to achieve better understanding of large annihilation rates observed for many polyatomic molecules [1–4]. In particular, we use an exactly solvable model to verify the prediction [5,6] that positron capture into vibrational Feshbach resonances (VFR) gives rise to a strong enhancement of the annihilation rate. We also use this model to investigate the dependence of positron binding energy for polyatomics on the size of the molecule. Such binding was postulated in [5,6] as a necessary condition for VFRs.

The annihilation rate for positrons in a gas of atoms or molecules can be expressed in terms of an effective number of electrons, $Z_{\rm eff}$, by

$$\lambda = \pi r_0^2 c Z_{\rm eff} n, \tag{1}$$

where r_0 is the classical electron radius, c is the speed of light and n is the number density of the gas. Measurements by Paul and Saint-Pierre in the early sixties [1] indicated unusually large positron annihilation rates in certain polyatomic molecular gases, with $Z_{\rm eff}$ exceeding the actual number of electrons by orders of magnitude. They speculated that this might be caused by the formation of positron–molecule bound states, and later Smith and Paul [7] explored the possibility that the large rates might be caused by a vibrational resonance. Research on the alkanes and similar molecules since that time [2–4] uncovered a rapid growth of $Z_{\rm eff}$ with the size of the molecule and very strong chemical sensitivity of $Z_{\rm eff}$. However, only recently a verisimilar physical picture of this phenomenon has begun to emerge [5,6,8]. These papers put forward a mechanism which is operational for molecules with positive positron affinities, and which involves capture of positrons into VFRs.

Recent measurements of annihilation with a positron beam at high resolution (25 meV) [9,10], have shown resonances in the energy dependence of the annihilation rate parameter, $Z_{\rm eff}$, of alkane molecules. Most of the features observed have been unambiguously identified as related to molecular vibrations. In particular, for all alkanes heavier than methane $Z_{\rm eff}$ displays a prominent C–H stretch vibrational peak. The experiments found that the magnitude of

* Corresponding author. Tel.: +44 28 9097 3161; fax: +44 28 9023 9182.
E-mail addresses: g.gribakin@qub.ac.uk (G.F. Gribakin), c.lee@qub.ac.uk (C.M.R. Lee).

0168-583X/$ - see front matter © 2006 Elsevier B.V. All rights reserved.
doi:10.1016/j.nimb.2006.01.035

$Z_{\rm eff}$ in the peak increases rapidly with the size of the molecule (similarly to the increase in $Z_{\rm eff}$ observed with thermal room-temperature positrons [2–4]). Another remarkable finding concerns the position of the C–H peak. While for ethane its energy is close to the mode energy of C–H stretch vibrations (0.37 eV), for heavier alkanes the resonances appear at an energy ~20 meV lower for each carbon added. This downward shift provides evidence of positron binding to molecules. The binding energies observed increase from about 14 meV in C_3H_8 to 205 meV in $C_{12}H_{26}$. Very recent experiments show evidence of a second bound state for alkanes with 12 and 14 carbons [11].

So far, realistic molecular calculations have not been able to reproduce enhanced $Z_{\rm eff}$. For hydrocarbons and a number of other polyatomics, calculations have been done using a model positron–molecule correlation potential in a fixed nuclei approximation [12,13]. Such calculations often provide a reasonable description of low-energy positron–molecule scattering. However, their results, almost without exception, underestimate experimental $Z_{\rm eff}$, in some cases by an order of magnitude. This suggests that to describe enhanced $Z_{\rm eff}$, dynamical coupling to molecular vibrations must be included. Such coupling was considered earlier for diatomics and CO_2 [14,15], where it had a relatively small effect on $Z_{\rm eff}$. (These molecules most likely do not form bound states with the positron, and do not possess VFR.) Calculations by the Schwinger multichannel method [16], which treats electron–positron correlations ab initio for fixed nuclei, also underestimate $Z_{\rm eff}$ for molecules such as C_2H_4 [17] and C_2H_2 [18] by an order of magnitude [19].

To examine the effect of vibrations on positron scattering and annihilation, we consider a simple model of Kr_2 dimer using the zero-range potential (ZRP) method [20]. In this model the interaction of the positron with each of the atoms is parameterised using the atomic value of the scattering length. It is applicable at low energies when the de Broglie wavelength of the projectile is much larger than the typical size of the scatterers. Once ZRP is adopted, the problem of the positron–molecule interaction, including the vibrational dynamics, can be solved practically exactly. In the previous paper [21] the interaction between the atoms in the dimer was treated using the harmonic approximation (HA), which allowed the vibrational coupling matrix elements to be calculated analytically. A parabolic potential does not describe well the shallow asymmetric interatomic potential for a weakly bound van der Waals molecule such as Kr_2. In this work we use the Morse potential to provide a better description of the molecular interaction. It is a good approximation to the best potential available for Kr_2 [22]. We examine how the use of a realistic molecular potential affects the positions and magnitudes of the VFR. To explore positron binding to polyatomics we again use the ZRP method. Specifically, we model alkanes by representing the CH_2 and CH_3 groups by ZRPs. We investigate the dependence of the binding energy on the number of monomers and find that a second bound state emerges for a molecule with ten carbons.

2. Zero-range model for a molecular dimer

In a van der Waals molecule the atoms are far apart and are only weakly perturbed by each other. This makes it an ideal system for applying the ZRP method. In this work we model the interaction between the two Kr atoms using the Morse potential (MP)

$$U(R) = U_{\rm min}\left[{\rm e}^{-2\alpha(R-R_0)} - 2{\rm e}^{-\alpha(R-R_0)}\right] \tag{2}$$

with the parameters $R_0 = 7.56$ a.u., $U_{\rm min} = 6.32\times10^{-4}$ a.u. $= 17.2$ meV and $\omega = (2U_{\rm min}\alpha^2/m)^{1/2} = 1.1\times10^{-4}$ a.u. $=$ 2.99 meV [23,24], where m is the reduced mass of Kr_2. The energy eigenvalues and eigenfunctions of the MP are given by simple analytical formulae [25]. In Fig. 1, we compare the Morse potential to an accurate fit of the best available Kr_2 potential [22]

$$V(R) = A{\rm e}^{-\alpha R-\beta R^2} - \sum_{n=3}^{8} f_{2n}(R,b)\frac{C_{2n}}{R^{2n}}, \tag{3}$$

where α, β and A characterise the short-range part of the potential, and C_{2n} is a set of six dispersion coefficients. The function $f_{2n}(R,b)$ is the damping function [26]

$$f_{2n}(R,b) = 1 - {\rm e}^{-bR}\sum_{k=0}^{2n}\frac{(bR)^k}{k!}. \tag{4}$$

The values of the parameters given in [22] are $\alpha = 1.43158$, $\beta = 0.031743$, $A = 264.552$, $b = 2.80385$, $C_6 = 144.979$, $C_8 = 3212.89$, $C_{10} = 92633.0$, $C_{12} = 3.57245\times10^6$, $C_{14} = 1.79665\times10^8$ and $C_{16} = 1.14709\times10^{10}$ (atomic units are used throughout).

Fig. 1 shows that the Morse potential is close to the best Kr_2 potential, while the HA is valid only in the vicinity of the minimum. This conclusion is supported by the comparison of the vibrational spacings. For the MP we have

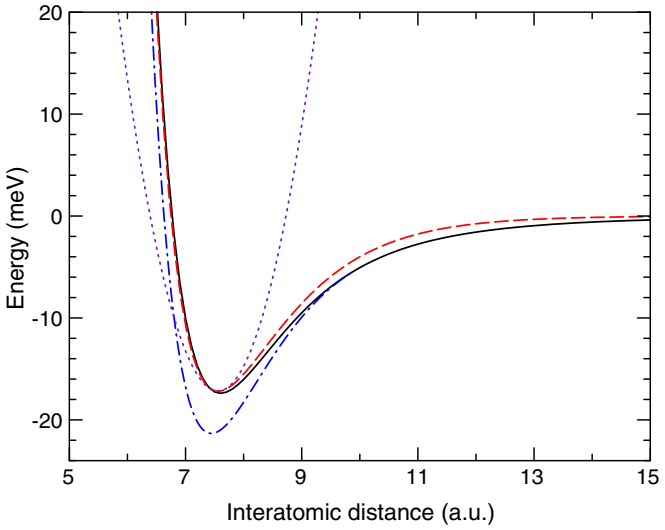

Fig. 1. Comparison of the best Kr_2 potential (solid curve) with the Morse potential (dashed curve) and harmonic approximation (dotted curve). Chain curve is the adiabatic potential for the e^+Kr_2.

$\omega_{10} \equiv E_1 - E_0 = 2.74$ meV, $\omega_{21} = 2.47$ meV, $\omega_{32} = 2.21$ meV, which agree well with $\omega_{10} = 2.65$ meV, $\omega_{21} = 2.39$ meV, $\omega_{32} = 2.12$ meV for the Kr_2 potential [22]. Both potentials are strongly anharmonic, with $\omega_{n+1,n}$ deviating markedly from $\omega = 2.99$ meV of HA. Obviously, the MP is a much better approximation than HA for modelling the Kr_2 potential.

In the ZRP model the interaction between a positron and an atom is expressed as a boundary condition for the positron wavefunction ψ

$$\frac{1}{r\psi}\frac{\mathrm{d}(r\psi)}{\mathrm{d}r}\bigg|_{r\to 0} = -\kappa_0, \tag{5}$$

where κ_0 is the reciprocal of the scattering length [20]. Positron–Kr scattering calculations yield $\kappa_0 = -0.1$ a.u. [27–29]. When applied to a two-centre problem, this condition can be expressed as

$$\Psi|_{\mathbf{r}\to\mathbf{R}_i} \simeq \text{const} \times \left(\frac{1}{|\mathbf{r}-\mathbf{R}_i|} - \kappa_0\right), \tag{6}$$

where $\mathbf{r}$ is the positron coordinate, and $\mathbf{R}_i$ $(i = 1, 2)$ are the coordinates of the two atoms.

Outside the (zero) range of action of the atomic potentials, the positron–dimer wavefunction can be written as a linear combination of the incident and scattered waves

$$\Psi = \mathrm{e}^{\mathrm{i}\mathbf{k}_0\cdot\mathbf{r}}\Phi_0(\mathbf{R}) + \sum_n A_n\Phi_n(\mathbf{R})\frac{\mathrm{e}^{\mathrm{i}k_n|\mathbf{r}-\mathbf{R}_1|}}{|\mathbf{r}-\mathbf{R}_1|} + \sum_n B_n\Phi_n(\mathbf{R}) \times \frac{\mathrm{e}^{\mathrm{i}k_n|\mathbf{r}-\mathbf{R}_2|}}{|\mathbf{r}-\mathbf{R}_2|}, \tag{7}$$

where $\mathbf{k}_0$ is the incident positron momentum, Φ_n is the nth vibrational state of the molecule $(n = 0, 1, \ldots)$, and $\mathbf{R} = \mathbf{R}_1 - \mathbf{R}_2$ is the interatomic distance. Eq. (7) is written for the case when the positron collides with a ground-state molecule. The coefficients A_n and B_n determine the excitation amplitude of the nth vibrational state of the molecule, and $k_n = [k_0^2 - 2(E_n - E_0)]^{1/2}$ is the corresponding positron momentum.

Applying (6) gives a set of linear equations for A_n and B_n

$$(\kappa_0 + \mathrm{i}k_n)A_n + \sum_m \left(\frac{\mathrm{e}^{\mathrm{i}k_m R}}{R}\right)_{nm} B_m = -(\mathrm{e}^{\mathrm{i}\mathbf{k}_0\cdot\mathbf{n}R/2})_{n0}, \tag{8}$$

$$(\kappa_0 + \mathrm{i}k_n)B_n + \sum_m \left(\frac{\mathrm{e}^{\mathrm{i}k_m R}}{R}\right)_{nm} A_m = -(\mathrm{e}^{-\mathrm{i}\mathbf{k}_0\cdot\mathbf{n}R/2})_{n0}, \tag{9}$$

where $\mathbf{n}$ is a unit vector along the molecular axis (whose direction we assume to be fixed during the collision), and the matrix elements are given by

$$\left(\mathrm{e}^{\pm\mathrm{i}\mathbf{k}_0\cdot\mathbf{n}R/2}\right)_{n0} = \int \Phi_n^*(R)\mathrm{e}^{\pm\mathrm{i}\mathbf{k}_0\cdot\mathbf{n}R/2}\Phi_0(R)\mathrm{d}R, \tag{10}$$

$$\left(\frac{\mathrm{e}^{\mathrm{i}k_m R}}{R}\right)_{nm} = \int \Phi_n^*(R)\frac{\mathrm{e}^{\mathrm{i}k_m R}}{R}\Phi_m(R)\mathrm{d}R. \tag{11}$$

In HA these matrix elements can be evaluated analytically, (10) – exactly, and (11) in the leading order [21]. For the MP we calculated them numerically.

After solving Eqs. (8) and (9) for A_n and B_n, one finds the total elastic $(0 \to 0)$ and vibrational excitation $(0 \to n$, $n = 1, 2, \ldots)$ cross-sections,

$$\sigma_{0\to n} = 4\pi\frac{k_n}{k_0}|A_n + B_n|^2 \tag{12}$$

and the positron annihilation rate,

$$Z_{\mathrm{eff}} = Z_{\mathrm{eff}}^{(0)}\kappa_0^2\sum_n(|A_n|^2 + |B_n|^2), \tag{13}$$

where $Z_{\mathrm{eff}}^{(0)}$ is the positron–atom Z_{eff} at $k = 0$ (see [21] for details). For Kr we use $Z_{\mathrm{eff}}^{(0)} = 81.6$ [27]. Eqs. (8) and (9) also allow one to determine the energies of bound states of the positron–dimer system, by looking for the poles of A_n and B_n at negative projectile energies, i.e. for imaginary positron momenta $k_0 = \mathrm{i}|k_0|$.

For doing numerical calculations, the set of Eqs. (8) and (9) can be truncated by assuming that $A_n = B_n = 0$ for $n > N_c$. This means that only the first $N_c + 1$ channels with $n = 0, 1, \ldots, N_c$ are taken into consideration. At low projectile energies only a small number of channels are open, and one obtains converged results with a relatively small N_c. In the calculations we used $N_c = 15$ and 10, for the HA and MP, respectively. This value for MP is the total number of bound excited states.

In the single-channel approximation, $N_c = 0$, the HA results practically coincide with those of the fixed-nuclei approximation, since the matrix elements (10) and (11) become $\mathrm{e}^{\pm\mathrm{i}\mathbf{k}_0\cdot\mathbf{n}R_0/2}$ and $\mathrm{e}^{\mathrm{i}k_m R_0}/R_0$, respectively (neglecting the second-order and higher corrections in the small parameter $k_0(m\omega)^{-1/2}$ [21]). A similar calculation for MP produces slightly different results, because of the asymmetry of the vibrational ground-state wavefunction, which gives rise to first-order corrections to these matrix elements.

3. Results for Kr_2

Table 1 shows the energies of the bound states (negative) and the VFRs (positive) of the e^+Kr_2 complex obtained with MP and in HA. In the $N_c = 0$ approximation the binding energies are $\varepsilon_0 = -3.77$ meV and $\varepsilon_0 = -3.48$ meV for HA and MP, respectively. The binding energy for the MP is smaller due to the asymmetry of the potential curve. The corresponding energies obtained from a multichannel calculation given in Table 1 are lower, because allowing the nuclei to move leads to stabilisation of the e^+Kr_2 complex.

Table 1
Energies of the bound states and resonances for e^+Kr_2

Level	Energy (meV)	
	HA	MP
0	−4.23	−3.89
1	−1.41	−0.74
2	1.42	2.16
3	4.25	4.83

The ground-state energy of the complex can also be compared to the results of an adiabatic calculation. For fixed nuclei the energy of the positron bound state is $-\kappa^2/2$, where κ is a positive root of the equation $\kappa = \kappa_0 + e^{-\kappa R}/R$. Adding this energy to the Kr_2 potential, one obtains the adiabatic potential for the e^+Kr_2 complex (chain curve in Fig. 1). Its minimum is about 3.94 meV below that of the Kr_2, which is close to the MP value of ε_0 in Table 1.

The first vibrational excitation energy of the e^+Kr_2 complex, $\omega'_{10} = \varepsilon_1 - \varepsilon_0$, for MP is 3.15 meV, while in HA it is 2.82 meV. Thus, MP calculations predict a "stiffening" of the vibrational motion of the complex in comparison with that of Kr_2. This effect is caused by a shift of the equilibrium position of the atoms to the left (see Fig. 1), towards the steep repulsive part of the interatomic potential. Note that in MP, the 2nd bound state with $\varepsilon_1 = -0.74$ meV lies just below the threshold. We will see that this causes a steep rise in $\sigma_{0\to0}$ and $Z_{\rm eff}$ as $k \to 0$. In HA this bound state is lower, i.e. further away from threshold, and its effect on the cross-sections is less noticeable. This combination of a lower binding energy and a greater vibrational frequency in MP, means that the first resonance observed in the cross-sections and in $Z_{\rm eff}$ will be at a greater energy than in HA.

Fig. 2 shows the elastic and vibrational excitation cross-sections obtained from Eq. (12) for MP and in HA. To highlight the effect of resonances, the elastic scattering cross-section has been calculated in both multichannel and single-channel ($N_c = 0$) approximations. The single-channel (fixed nuclei) elastic cross-sections from the two calculations are quite close. The multichannel cross-sections are qualitatively similar, the main difference being in the positions and widths of the resonances and energies of the vibrational thresholds. The magnitudes of the $\sigma_{0\to1}$ and $\sigma_{0\to2}$ cross-sections are greater for MP. Another noticeable difference is in the rise of $\sigma_{0\to0}$ towards zero positron energy in MP calculation.

Fig. 3 shows the positron annihilation rate (13) obtained with and without the coupling to the vibrational motion, i.e. from the multichannel and single-channel calculations. The background ("fixed nuclei", $N_c = 0$) $Z_{\rm eff}$ at low positron momenta is enhanced due to the large positron-Kr_2 scattering length. Such enhancement first predicted in [30], affects both $Z_{\rm eff}$ and the elastic cross-section, which in this case are proportional to each other, $Z_{\rm eff} \sim \sigma_{\rm el}/4\pi$ in atomic units [5,6]. The effect of VFRs on $Z_{\rm eff}$ is much more prominent than in scattering, with the strongest resonance four orders of magnitude above the background. The widths of the resonances in MP and HA, are quite different, e.g. $\Gamma = 2.8$ μeV (MP) versus $\Gamma = 16.7$ μeV (HA) for the strongest $n = 2$ resonance. This difference, also seen in the scattering cross-sections (Fig. 2), means that anharmonicity of the Kr_2 potential reduces the coupling between the incident positron and vibrationally-excited e^+Kr_2 compound. A possible explanation for this is that for MP, positron binding has only a small effect on the equilibrium position of the nuclei (as seen from the adiabatic potential curve of e^+Kr_2 in Fig. 1).

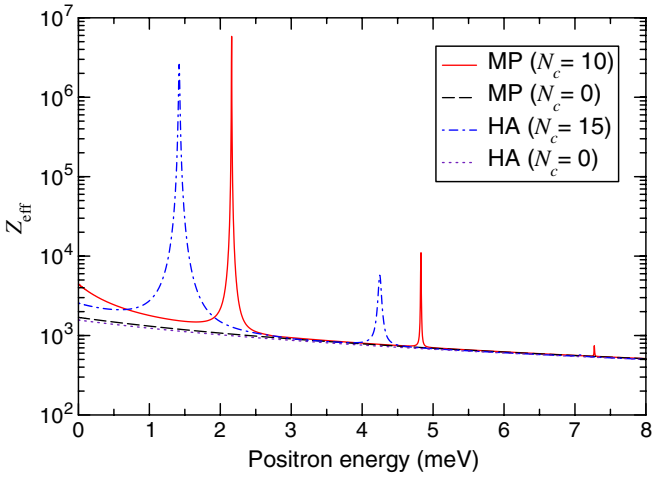

Fig. 3. $Z_{\rm eff}$ for positrons on Kr_2 calculated using MP and HA in the multichannel (solid and chain curves, respectively) and single-channel (dashed and dotted curves, respectively) approximations.

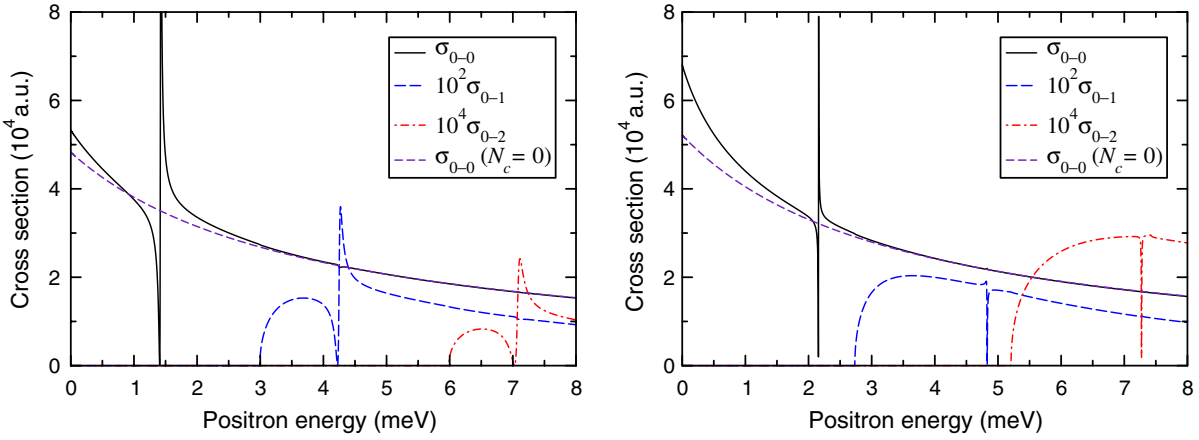

Fig. 2. Cross-sections for positron scattering from Kr_2 calculated using HA (left) and MP (right): solid curve, elastic scattering, $\sigma_{0\to0}$; long-dashed curve, vibrational excitation, $\sigma_{0\to1}$ (times 10^2); chain curve, vibrational excitation, $\sigma_{0\to2}$ (times 10^4); short-dashed curve, single-channel elastic cross-section.

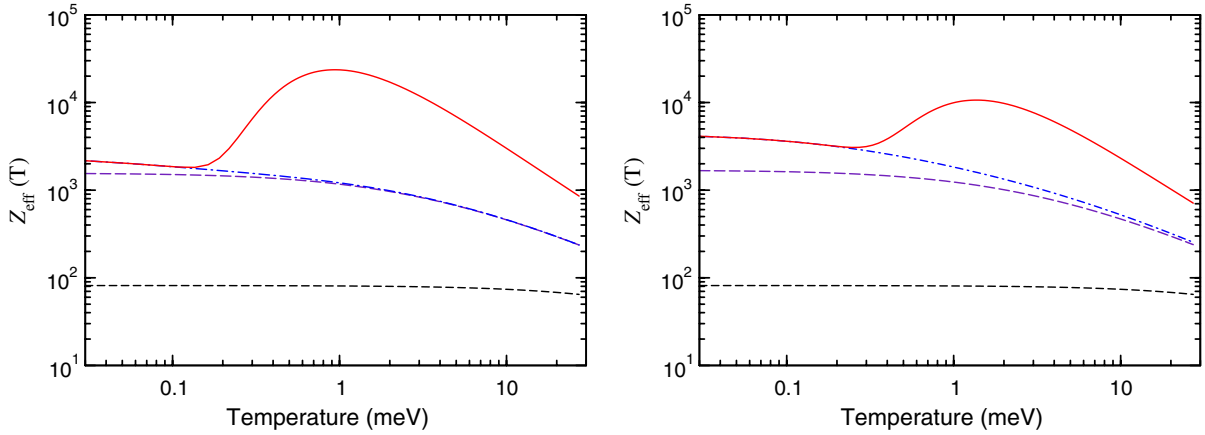

Fig. 4. Thermally averaged $Z_{\rm eff}$ for positrons on Kr_2, obtained using HA (left) and MP (right): long-dashed curve, single-channel approximation; chain curve, multichannel calculation, non-resonant background; solid curve, multichannel calculation, total, including the VFR. For comparison, $Z_{\rm eff}$ for Kr is shown (short-dashed curve).

To compare the integral contribution of the resonances, we averaged $Z_{\rm eff}$ over the Maxwellian positron energy distribution

$$\bar{Z}_{\rm eff}(T) = \int_0^\infty Z_{\rm eff}(k) \frac{{\rm e}^{-k^2/2k_{\rm B}T}}{(2\pi k_{\rm B}T)^{3/2}} 4\pi k^2 \, {\rm d}k. \qquad (14)$$

Fig. 4 shows $\bar{Z}_{\rm eff}(T)$ for HA and MP. In both cases the VFR gives a very large contribution, increasing $Z_{\rm eff}$ by an order of magnitude at $T \sim 1$ meV, i.e. for positron energies close to that of the resonance. Its effect is seen even at much higher temperatures, raising $Z_{\rm eff}$ above the non-resonant background by a factor of three for room temperature positrons.

4. ZRP model of positron binding to polyatomics

In positron–molecule collisions VFRs occur when the energy of the incident positron plus the energy released in positron–molecule binding, equals the energy of a vibrational excitation of the positron–molecule complex. For weakly bound positron states the latter should be close to a vibrational excitation energy of the neutral molecule. Hence, by observing VFRs one can obtain information on the binding energy. This procedure was applied to electron scattering from $(CO_2)_N$ clusters [31]. In this system the redshift of the VFR was found to increase with the cluster size by about 12 meV per unit. A simple model of a spherically-symmetric cluster with a constant potential inside and $-\alpha e^2/2r^4$ potential outside was able to reproduce the dependence of the electron binding energy on the cluster size.

For positrons, the measurements of the energy dependence of $Z_{\rm eff}$ for alkanes with a high-resolution positron beam allow one to determine their positron binding energies [9,10]. However, an accurate ab initio calculation of positron binding to a polyatomic molecule is probably beyond the capability of present-day theory. Even for atoms, calculations of positron binding remain a challenging task because of the need to carefully account for strong electron–positron and many-electron correlations (see, e.g. [32]).

In this work we have adopted a different approach. To examine positron binding to alkanes, we model the molecule by representing each CH_2 or CH_3 group by a ZRP centred on the corresponding carbon atom. The wave function of a bound state decreases as $r^{-1}{\rm e}^{-\kappa r}$ at large positron–molecule separation r, where $\kappa^2/2$ is the binding energy. For weakly bound states this wavefunction is very diffuse ($\kappa \ll 1$ a.u.), which means that the positron moves mostly far away from the molecule. The actual binding energy is determined by their interaction at small distances, and the ZRP model is a simple way of parametrizing such interaction. It allows us to account for the scaling of the positron–molecule interaction with the number of monomers (to the extent that the monomers do not have a large effect on each other), and to use a realistic geometry of the molecule. We will consider two cases, a straight carbon chain (Fig. 5(a)) and a "zigzag" carbon chain (Fig. 5(b)) which matches the actual structure of the molecule (Fig. 5(c)). Unlike the Kr_2 model, the κ_0 parameter of the ZRP for alkanes is adjusted semiempirically (see below).

The bound-state positron wavefunction in the field of N ZRP centres has the form [20],

$$\Psi = \sum_{i=1}^{N} A_i \frac{{\rm e}^{-\kappa|\mathbf{r}-\mathbf{R}_i|}}{|\mathbf{r}-\mathbf{R}_i|}. \qquad (15)$$

Subjecting it to N boundary conditions (6) with parameters κ_{0i}, we find the positron energy as $\varepsilon_0 = -\kappa^2/2$, where κ is a positive root of the equation

$$\det\left[(\kappa_{0i}-\kappa)\delta_{ij} + \frac{{\rm e}^{-\kappa R_{ij}}}{R_{ij}}(1-\delta_{ij})\right] = 0. \qquad (16)$$

Here $R_{ij} = |\mathbf{R}_i - \mathbf{R}_j|$ is the distance between the ith and jth ZRP.

For modelling alkanes we choose the distance between the neighbouring ZRPs equal to the length of the C–C

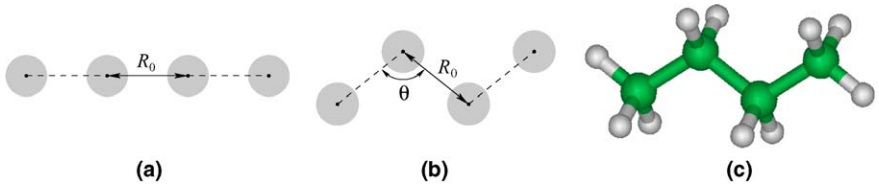

Fig. 5. Zero-range potential models of the alkane molecule (butane, C_4H_{10}, is shown). In (a) and (b) the shaded circles represent a CH_2 or CH_3 group, while (c) is a true 3D molecular structure [33]. The parameters used are $R_0 = 2.911$ a.u. and $\theta = 113°$.

bond. All ZRPs are characterised by the same value of $\kappa_{0i} = -1.5$. This value ensures that the molecule with three ZRP centres (which models propane, C_3H_8) has a small binding energy, 7 meV for the straight chain, and 12 meV for the zigzag chain. These values are close to that inferred from experiment [9,10], where propane is the first molecule for which a downshift of the C–H peak from the corresponding vibrational energy can be seen [9,10].

In Fig. 6 the results of our calculations are compared with the experimental binding energies. As we move from a straight ZRP chain (Fig. 5(a)) to a "zigzag" chain (Fig. 5(b)) the binding energy increases. This is expected as the carbon atoms beyond the nearest neighbour become closer to each another. The overall dependence of the binding energy on the number of monomers n predicted by the ZRP model is similar to that of the experimental data, while the absolute values predicted by our simple theory are within a factor of two of the measurements. One may also notice that the measured binding energies increase almost linearly with n, while the calculation shows signs of saturation. These discrepancies might be related to the fact that the ZRP model disregards the long-range $-\alpha e^2/2r^4$ nature of the positron–molecule interaction, which would restrict its validity to very small binding energies.

A remarkable feature of the model calculations is the emergence of a second bound state for $n = 10$ in both straight and "zigzag" chains. This prediction supports the experimental evidence for the second bound state, in the form of a C–H peak, which re-emerges at 0.37 eV for dodecane ($n = 12$) [9,10] and stabilises by about 50 meV for $C_{14}H_{30}$ [11].

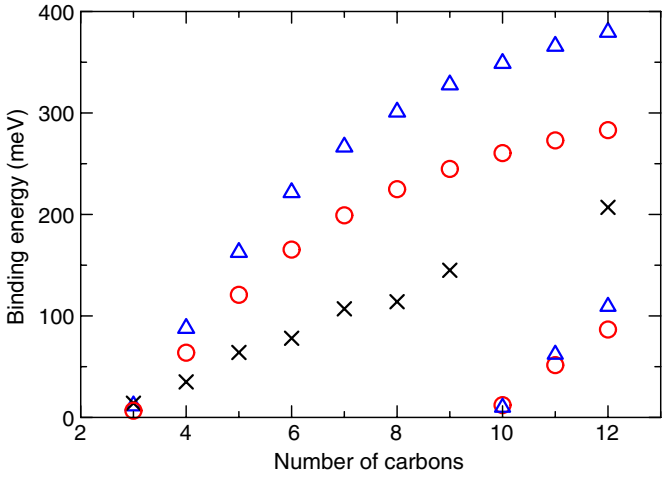

Fig. 6. Positron binding energies $|\varepsilon_0|$ for alkanes modelled using straight (circles) and "zigzag" (triangles) ZRP chains. Experimental results (crosses) [9,10] are shown for comparison.

5. Summary and outlook

We have used the Morse potential to model the interaction between the atoms in the Kr_2 dimer. We find that the positron binding energies and the positions and widths of the VFR change compared with the harmonic approximation. However, the overall picture remains similar, with the lowest VFR enhancing the Maxwellian-averaged positron annihilation rate by an order of magnitude to $Z_{\rm eff} \sim 10^4$ at $T \sim 1$ meV.

In principle, a similar approach could be applied to positron interaction with other rare-gas dimers and clusters. For Ar and lighter atoms, the positron–atom attraction is too weak to allow formation of positron bound states and VFRs. For Xe_2, on the contrary, the attraction is much stronger ($\kappa_0 \sim -0.01$ [28]). This leads to a much greater positron–dimer binding energy (~40 meV), which means that many vibrationally excited states of e^+Xe_2 are bound, and only those with high n lie above the positron–dimer continuum threshold. The coupling between these states and the target ground state is extremely weak, and we have not been able to find any VFR for positrons incident on ground-state Xe_2 in our calculations.

A zero-range potential model for positron binding to alkanes yields binding energies that are in qualitative agreement with experiment. Our calculation predicts the emergence of the second bound state for a molecule with ten carbon atoms. Such a bound state may have already been observed for dodecane and tetradecane.

Zero-range potential is an exceptionally simple model. The accuracy of our predictions is of course limited by the nature of the ZRP model. In particular, ZRPs disregard the long-range character of the positron-target polarisation attraction. This is a reasonable approximation for very weakly bound states, but as the binding gets stronger, larger errors may be introduced. Given the difficulty of performing ab initio calculations for positron interaction with polyatomics, one hopes that more sophisticated yet tractable models could be developed. They should provide a more accurate description of positron–molecule binding and capture into vibrational Feshbach resonances. One may then hope to fully explain the dramatic enhancement

of the annihilation rates and their strong chemical sensitivity for polyatomic molecules.

Acknowledgements

We are grateful to L.D. Barnes, C.M. Surko and J.A. Young for drawing our attention to the experimental evidence for a second positron bound state for larger alkanes.

References

[1] D.A.L. Paul, L. Saint-Pierre, Phys. Rev. Lett. 11 (1963) 493.
[2] G.R. Heyland, M. Charlton, T.C. Griffith, G.L. Wright, Can. J. Phys. 60 (1982) 503.
[3] C.M. Surko, A. Passner, M. Leventhal, F.J. Wysocki, Phys. Rev. Lett. 61 (1988) 1831.
[4] K. Iwata, R.G. Greaves, T.J. Murphy, M.D. Tinkle, C.M. Surko, Phys. Rev. A 51 (1995) 473.
[5] G.F. Gribakin, Phys. Rev. A 61 (2000) 022720.
[6] G.F. Gribakin, in: C.M. Surko, F. Gianturco (Eds.), New Directions in Antimatter Chemistry and Physics, Kluwer Academic Publishers, Netherlands, 2001, p. 413.
[7] P.M. Smith, D.A.L. Paul, Can. J. Phys. 48 (1970) 2984.
[8] G.F. Gribakin, P.M.W. Gill, Nucl. Instr. and Meth. B 221 (2004) 30.
[9] S.J. Gilbert, L.D. Barnes, J.P. Sullivan, C.M. Surko, Phys. Rev. Lett. 88 (2002) 043201.
[10] L.D. Barnes, S.J. Gilbert, C.M. Surko, Phys. Rev. A 67 (2003) 032706.
[11] L.D. Barnes, J.A. Young, C.M. Surko, private communication, 2005.
[12] F.A. Gianturco, T. Mukherjee, A. Occhigrossi, Phys. Rev. A 64 (2001) 032715.
[13] A. Occhigrossi, F.A. Gianturco, J. Phys. B 36 (2003) 1383.
[14] F.A. Gianturco, T. Mukherjee, Europhys. Lett. 48 (1999) 519.
[15] F.A. Gianturco, T. Mukherjee, Nucl. Instr. and Meth. B 171 (2000) 17.
[16] E.P. da Silva, J.S.E. Germano, M.A.P. Lima, Phys. Rev. A 49 (1994) R1527.
[17] E.P. da Silva, J.S.E. Germano, M.A.P. Lima, Phys. Rev. Lett. 77 (1996) 1028.
[18] C.R.C. de Carvalho, M.T. do, N. Varella, M.A.P. Lima, E.P. da Silva, J.S.E. Germano, Nucl. Instr. and Meth. B 171 (2002) 33.
[19] M.T. do, N. Varella, C.R.C. de Carvalho, M.A.P. Lima, Nucl. Instr. and Meth. B 192 (2002) 225.
[20] Yu.N. Demkov, V.N. Ostrovsky, Zero-Range Potentials and their Applications in Atomic Physics, Plenum Press, New York, 1988.
[21] G.F. Gribakin, Nucl. Instr. and Meth. B 192 (2002) 26.
[22] T.P. Haley, S.M. Cybulski, J. Chem. Phys. 119 (2003) 5487.
[23] A.A. Radtsig, B.M. Smirnov, Parameters of Atoms and Atomic Ions: Handbook, Energoatomizdat, Moscow, 1986 (in Russian).
[24] K.P. Huber, G. Herzberg, Constants of Diatomic Molecules, van Nostrand Reinhold, New York, 1979.
[25] L.D. Landau, E.M. Lifshitz, Quantum Mechanics, third ed., Pergamon, Oxford, 1977.
[26] K.T. Tang, J.P. Toennies, J. Chem. Phys. 80 (1984) 3726.
[27] R.P. McEachran, A.D. Stauffer, L.E.M. Campbell, J. Phys. B 13 (1980) 1281.
[28] V.A. Dzuba, V.V. Flambaum, G.F. Gribakin, W.A. King, J. Phys. B 29 (1996) 3151.
[29] J. Ludlow, Ph.D. Thesis, Queen's University, Belfast, 2003.
[30] V.I. Goldanskii, Yu.S. Sayasov, Phys. Lett. 13 (1964) 300.
[31] E. Leber, S. Barsotti, I.I. Fabrikant, J.M. Weber, M.W. Ruf, H. Hotop, Eur. Phys. J. D 12 (2000) 125.
[32] J. Mitroy, M.W.J. Bromley, G.G. Ryzhikh, J. Phys. B 35 (2002) R81.
[33] K. Irikura, in: P.J. Linstrom, W.G. Mallard (Eds.), NIST Chemistry WebBook, NIST Standard Reference Database Number 69, June 2005, National Institute of Standards and Technology, Gaithersburg, MD 20899, Available from: <http://webbook.nist.gov>.